VALIDATION OF ENERGY BALANCE ESTIMATES FROM SNOW COVERED AREAS OF THE ANTARCTIC PENINSULA BASED ON ERS-PRI-IMAGES

Christoph Schneider, Stefan Wunderle, Hermann Gossmann, Helmut Saurer

Department of Physical Geography, Universität Freiburg
Werderring 4, D-79085 Freiburg, Germany

phone: +49-761-203-3548, fax: +49-761-203-3596, e-mail: chri@ipg.uni.freiburg.de

ABSTRACT

Two glaciers of the Antarctic Peninsula at 68° south were chosen to monitor snow cover properties using ERS-PRI images. Properties of the snow cover reflect local meteorological conditions. Therefore in order to detect climate variability on the basis of the seasonal dynamic of the snow, ERS images that show variations due to changes in the snow cover are utilised. During two summer seasons ERS-PRI data covering the area were collected. Simultaneously field measurements were accomplished in order to link up findings in the ERS images with observed meteorological conditions.
During the field campaigns micro-meteorological measurements with three automatic weather stations (AWS) were carried out on the glaciers. More than 40 snow pits were dug during the summer season to obtain ground truth data from the snow cover. Based on data from AWS the amount of energy available for melting was computed. The energy balance as derived for the locations of the AWS was than calculated for the entire surface area of the glaciers taking into account a digital terrain model (DTM) and a model for short-wave irradiance. The result can be used to separate periods and areas with melting from periods and areas with a completely frozen snow cover. The same separation can be achieved from the evaluation of ERS-1 imagery. The comparison of ERS derived snow property maps and maps modelled from ground truth data shows good agreement. Hence it is concluded that ERS-PRI data is a useful tool to monitor seasonal snow cover behaviour respectively local climate variations on the Antarctic Peninsula.

1. INTRODUCTION

Global circulation models (GCM) predict considerable warming for high latitude regions in respect to increasing amounts of green house gases in the atmosphere. However spatially distributed predictions of regional climate change suffer from insufficient resolution of the GCMs. It is therefore highly desirable to obtain methods for regional climate monitoring at high latitudes. Representation of climate behaviour along the Antarctic Peninsula located between 62° and 75° south (Fig. 1) as given by GCMs is very limited due to its small extension from east to west of only about 150 km. Nevertheless the region is of great interest for climate monitoring for a couple of reasons: Large gradients of mean annual temperature and precipitation rate both from west to east and from north to south along the Peninsula will lead to strong climatological effects as a reaction to a changing climate. Local sea ice extent greatly influences the climate conditions in the region because of the different energy balance of sea ice and open water. Hence long-term changes in annual sea ice extent will contribute considerable to local climate change. Glaciers in the coastal zones of the Antarctic Peninsula are much smaller than glacial systems in central parts of Antarctica. The response time of these small glaciers to climate change is only in the range of years to decades and changes due to regional climate variations will be much easier accessible than elsewhere in Antarctica. The impact of man on most parts of Antarctica is still negligible. It is therefore possible to attribute changes of local ecosystems to varying climate conditions without having to consider the impact of human behaviour.
While most meteorological time series from the Antarctic Peninsula show a warming trend the data is still not statistically significant because of the short time series available (Sanson, 1989). However ice shelves along the Peninsula have reduced considerably recently (Vaughan & Doake, 1996, Skvarca, 1993) backing climate change predictions. On the other hand the net of meteorological observations is coarse with only about 10 stations or AWS running permanently on the Antarctic Peninsula. Hence a method to support climate monitoring by means of remote sensing is of great interest. Remote sensing contributes spatially distributed information to the point meteorological time series obtained by ground measurements. SAR imagery such as the ERS-1/2-PRI-images can be used to separate areas with liquid water content in the snow cover from areas without liquid water content. This is due the different absorption and scattering behaviour of liquid water, ice and snow crystals. The backscatter coefficients typically found on horizontal areas of the investigated glaciers vary from -6 dB to -1 dB for dry snow with ice lenses and crystal sizes from 1 to 3 mm, while wet snow with some liquid water content leads to backscatter coefficients between -19 dB and -13 dB (WUNDERLE, 1996). Consequently the spatial and temporal location of the transition from wet to dry snow zone can be monitored with a time series of SAR

Proc. 3rd ERS Symp. on Space at the service of our Environment, *Florence, Italy, 17–21 March 1997* (ESA SP-414, 3 Vols., May 1997)

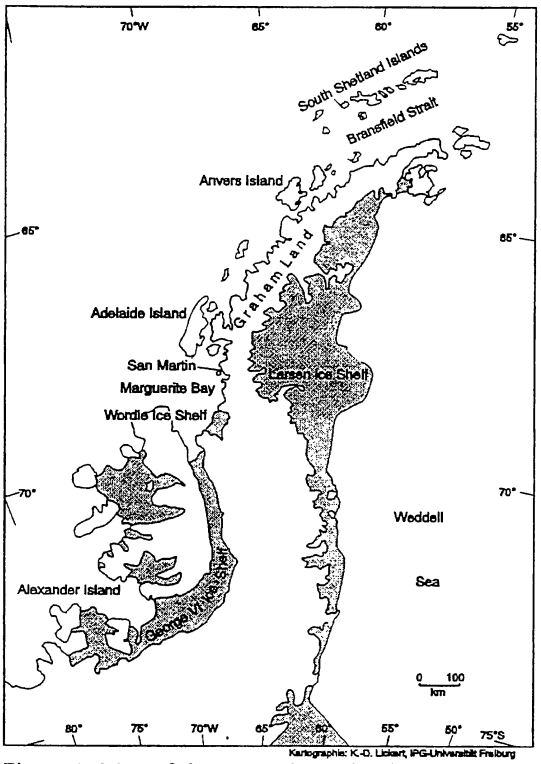

Figure 1. Map of the Antarctic Peninsula. The area of investigation is located in the vicinity of the Argentine Research Base 'San Martin'

images. This transition zone on the other hand varies according to meteorological fluctuations.
This investigation aims to develop a method to evaluate ERS-1-PRI imagery of the Antarctic Peninsula from January 1995 in respect to the meteorological situation on the observed glaciers. Energy budget and temperature gradients have been calculated from meteorological measurements. From this an actual transition between dry and wet snow zone was modelled and compared to the ERS-1 image.

2. AREAS OF INVESTIGATION

Two glaciers located at 68° south and 67° west on the west coast of the Antarctic Peninsula, in inner Marguerite bay were chosen for the investigation outlined above (Fig. 2). Both glaciers form a joined ice cliff to the sea and are easily accessible from the Argentine research base 'General San Martin' located in front of the ice cliff on a small, rocky island. McClary Glacier is a valley glacier with a small accumulation area reaching up to approximately 600 m a.s.l. The outflow of the ice is directed into two contrary directions (WU, THIEL & WUNDERLE, 1996). Northeast glacier, to the south of McClary Glacier, in contrary is a large valley glacier with a total length of about 25 km fed by an ice stream coming down from the plateau of the Antarctic Peninsula at approximately 1500 m a.s.l. Northeast-Glacier forms a piedmont-like ice lobe at sea-level. Both ice streams are flanked by ridges with summits at altitudes between 700 and 1000 m a.s.l. Because of the different glacial and topographic features it is anticipated that the glaciers react differently to regional climate variations.
The mean annual temperature at sea level is -5.5 °C but mean annual temperatures vary as much as +/-4 Kelvin. Mean temperatures in January range from -1.5°C to +2.5°C (REYNOLDS, 1981, SCHWERDTFEGER, 1976, WUNDERLE, 1996). When compared to other locations on the Antarctic Peninsula this region obtains much direct solar radiation and less precipitation because of the sheltered situation with high mountains to the north (Adelaide Island), east (Palmer Land) and south (Alexander Island).
With these climate conditions the equilibrium line of both glaciers is about at sea-level with superimposed ice being exposed occasionally. During summer the lower parts of the glaciers belong to the wet snow zone with considerable melting taking place approximately between sea level and 400 m a.s.l.

3. DATA

3.1 Field measurements

During the austral summer 1994/1995 field data was acquired. AWS supplied with 10 Watt solar panels were placed at three locations on the glaciers at different elevations measuring radiation, temperature, humidity, wind speed and wind direction. The data was stored as means of 10 minutes in a data logger. Further to this meteorological data from the adjacent Argentine research base 'General San Martin' could be used. More than 40 snow pit were dug to obtain data from the snow cover with both spatially and temporally distributed values. Some of the parameters observed were stratification, crystal type and crystal size, liquid water content and extent of ice lenses.

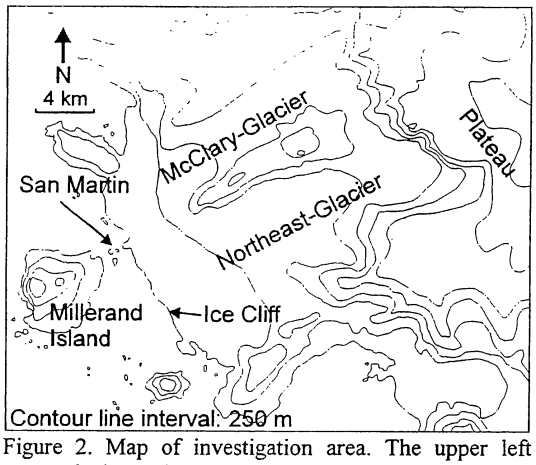

Figure 2. Map of investigation area. The upper left corner is located at 67°17'33'' west and 68°14'06'' south.

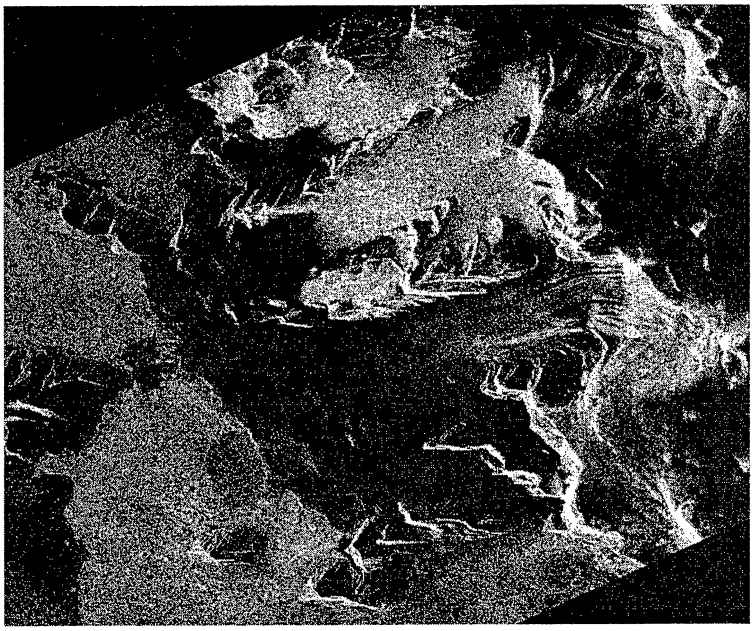

Figure 3. ERS-1 PRI image from 18.01.1995, 2:00 local time. The image depicts an area on the west coast of the Antarctic Peninsula at 68° South and 67° West. The plateau of Palmer Land can partly be seen at the eastern margin of the image. The central parts of the image are comprised by McClary-Glacier to the North and Northeast-Glacier to the South. The mountainous island to the East is Millerand Island. Bright areas on the north-western parts of McClary-Glacier are due to frozen snow interspersed with ice lenses. The low lying parts of McClary and the surface of Northeast glacier is depicted in dark tones signifying the presence of liquid water in the snow cover.

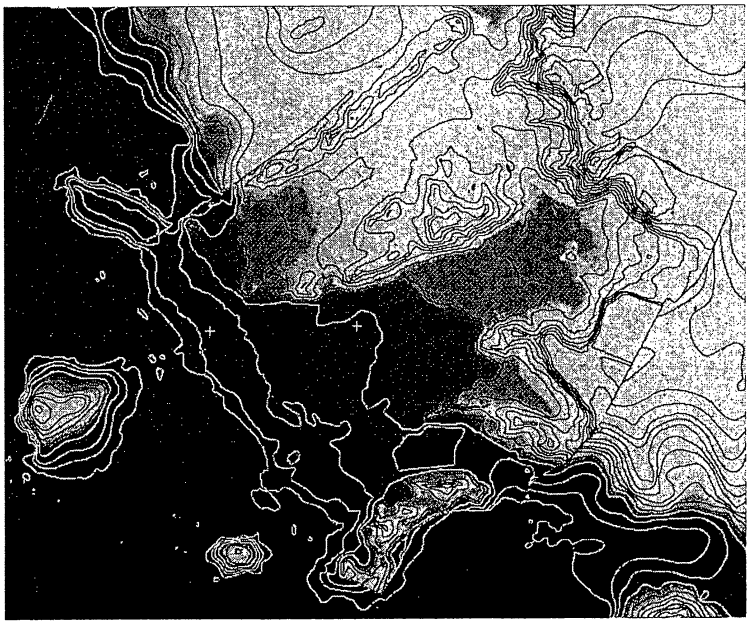

Figure 4. Model result for the time of image acquisition based on meteorological measurements and a simple snow cover model with 7 snow layers. Contour lines with 100m intervals as derived from the DTM are overlaid. Discontinuities at contour lines result from merging DTMs with different resolution. The crosses mark the locations of automatic weather stations. All areas with shaded grey tones represent areas with some liquid water content leading to reduced backscatter intensities on the SAR image. Only the lightest grey tone stands for areas with absolutely frozen snow and with no liquid water content at all.

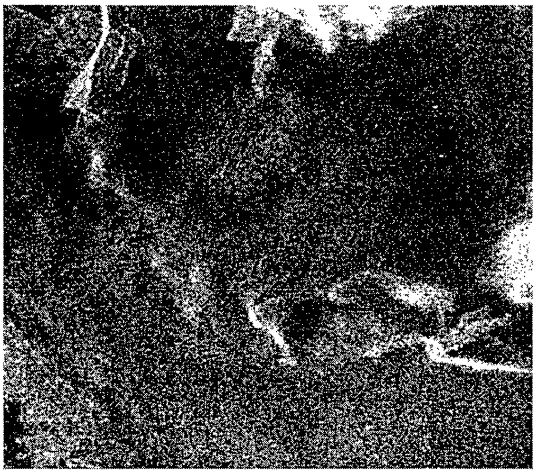

Figure 5. Subset from ERS-1-PRI image with white dots signifying the corner reflectors mounted on the glaciers. The reflectors were used to identify locations of AWS and to assess glacier motion at the surface.

3.2 ERS-1 SAR image

The ERS-1-SAR image was acquired at 02:00 local time on 18th January 1995 (Fig. 3). The surface of the sea along the left side of the image shows irregular patterns due to surface motion of the sea. Ice floes and icebergs contribute to this inhomogenous pattern. The ice cliff runs north-east south-west. The central areas of the image show the McClary-Glacier to the north and the Northeast-Glacier to the south. Both glaciers form the joined ice cliff, which faces south-west. The surfaces of the glaciers are softly undulating. The rather dark tone on the glacier surface adjacent to the ice cliff and on Northeast-Glacier is due to wet conditions in the snow cover. This leads to heavy absorption of the microwave radiation from the ERS-1. Further to the east, at higher altitudes on McClary Glacier, the transition to lighter tones can be observed. Here temperatures in the snow cover are well below zero and the absorption of the radiation decreases rapidly due to the almost total absence of liquid water in the snow cover. Consequently, the bright colour results from scattering at ice lenses and large snow grains in the snow cover (WUNDERLE & SAURER 1995).

On McClary Glacier three corner reflectors were installed to monitor the ice velocity and to identify the location of automatic weather stations. These reflectors can be identified as bright white spots in the upper right quarter of the subset presented in Fig. 5. An additional corner reflector is situated to the west of the ice cliff at the lower margin of the subset.

4. METHODOLOGY

AWS were operated at three locations on the glaciers marked with crosses in Fig. 5. The data acquired was used to compute sensible heat flux (H) and latent heat flux (LE) according to the bulk transfer equations. For a detailed derivation of these formulas see for example (BRUTSAERT, 1982). The heat fluxes were computed by

$$H = -\frac{\rho\kappa^2 c_p u(z)}{\left(\ln\frac{z}{z_0}\right)^2}(T(z) - T(0))(1 - 5Ri)^2$$

and

$$LE = -\frac{\rho \cdot 0.623 \cdot l_v \kappa^2 u(z)}{p\left(\ln\frac{z}{z_0}\right)^2}(e(z) - E(0))(1 - 5Ri)^2$$

with ρ air density, c_p the specific heat of air (1005 J/(kg*K)), κ van Karmen's constant (0.4), l_v latent heat of evaporation, T air temperature, e vapour pressure, E saturation vapour pressure, z elevation above snow surface, z_0 surface roughness length, p near surface air pressure and u wind speed. The effect of stable stratification in the atmosphere was taken into account using the bulk Richardson number given by (BRAITHWAITE, 1995),

$$Ri = -\frac{g\frac{\partial T}{\partial z}}{T\left(\frac{\partial u}{\partial z}\right)^2}$$

with g the acceleration due to gravity (0.981 m/s^2), as measure for correction of stability effects. Radiation balance was measured directly with Q-7 net radiometers by Campbell Scientific, UK With the snow cover being isothermal at 0° C in the upper most two meters during the summer, positive energy balance was assumed to be transformed to melt energy in the snow cover on situations with positive air temperature at screen level. On the basis of this approximation the amount of water equivalent removed from the top layer of the snow cover was calculated. This was correlated with the depletion of the snow as monitored in snow pits regularly dug at the sites of the AWS. The correlation coefficient r was found to be 0.92 (Fig. 6).

	Coefficient of regression	Explained variance
Temperature	9.971 W/m^2 / K	55 %
Irradiance	0.088 W/m^2 / W/m^2	37 %
Regression constant	3.097 W/m^2	
Multiple Reg. coefficient.		60 %

Table 1. Regression coefficients and explained variance for multiple regression analysis between temperature, solar irradiance and energy balance based on means of 6 hours.

The relationship between energy balance and meteorological parameters was further studied with statistical methods in order to derive spatially distributed data.

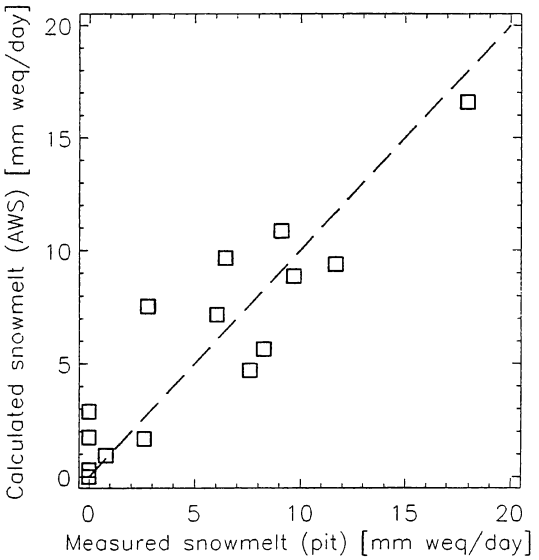

Figure 6. Correlation with r = 0.92 between measured and computed snowmelt in mm water-equivalent for the locations of the 3 AWS. Each rectangle represents a time period of several days.

Regression analysis of air temperature and solar irradiance as independent variables and energy balance as dependent variable turned out to be best when performed on the basis of means of six hours respectively four values per day. The regression coefficients are given in Tab. 1. Actual temperature gradients calculated from the AWS located at different altitudes were used to provide a data layer of air temperature for each quarter of each day. Short-wave irradiance was modelled employing the Short-wave-Irradiance-Model (SWIM), described in detail in PARLOW (1996). The effect of cloudiness was considered by computing the ratio between modelled and measured irradiance for the three locations of the AWS. Employing an interative approach this ratio was re-introduced into the modelling scheme of SWIM.

Using the coefficients of the multiple regression analysis as computed beforehand, the spatial data sets of temperature and irradiance were used to produce estimates of the spatial distribution of the energy balance for each quarter of a day. To separate dry and wet snow zone a simple snow cover model with seven layers of approximately 10 cm depth each was assumed. The idea of the model is to reduce the number of wet layers by one if air temperature and energy budget are negative at a given grid point and to do the opposite if both determining data sets show positive values for a grid point. If the snow cover is comprised by only dry layers nothing is changed in case of further cooling. After complete wetting of all seven layers of the upper snow cover this is not enhanced in case of further 'warming'. The snow cover model is optimised according to the local conditions characterised by a snow pack composed of highly metamorphosed snow grains of 1 to 3 mm diameters and interspersed ice lenses. ERS microwave radiation penetrates frozen snow with these properties to a depth of approximately 0.7 m (FRIEDRICH, 1996). However even small amounts of liquid water reduce the backscatter intensity significantly (FRIEDRICH, 1996). Therefore we assume that only a model result with all seven layers being completely frozen will result in bright tones on the ERS-1 image as found on the upper parts of McClary-Glacier on 18th January 1995. For all grid points with at least one layer containing liquid water a considerable reduction of the backscatter intensity as found on Northeast-Glacier on the same frame is forecasted.

5. MODEL RESULT

Fig. 4 represents the status of the model for the time of the satellite's overpass. Contour lines with 100 m intervals are overlaid. The discontinuities in the digital terrain model (DTM) originate from merging to different DTMs. The inner part with 40 m ground resolution and approximately 10 m of vertical accuracy was produced from aerial photography by the Institute of Applied Geodesy in Frankfurt, Germany, whereas the frame was derived from the British Antarctic Survey's 'Digital Database Antarctica' at a much lower resolution. The transition from wet to dry snow zone is modelled correctly for both glaciers. Even the wet snow zone on the outlet of McClary-Glacier to the north-east is modelled accordingly. Some discrepancy can be observed on the glacial bed to the north of McClary-Glacier. However this may be attributed to an inaccurate DTM in this area.

6. DISCUSSION AND CONCLUSIONS

The good agreement between model and SAR image for 18.01.1995 is a promising provisional result. Further efforts will have to address a couple of questions not yet firmly answered. A crucial point is the definition of the snow cover model and the accurate number of layers in the model. The process of wetting and freezing in the snow cover according to meteorological conditions is modelled very schematic instead of being based on physical modelling. It is assumed that every 6 hours a layer of approximately 10 cm is changed. This relation obviously is a rough estimate and varies both in time and in space. Furthermore we do not consider the time delay due to the slow heat conduction in the snow cover between changes occurring in the atmospheric boundary layer and the anticipated effects at deeper layers in the snow cover. These inherent simplifications need to be reconsidered. As a next step data from other time periods will have to be processed. Application of the model to other drainage basins would also be of great interest. In spite of the approximations that limit the accuracy greatly, the major advantage of this approach is to obtain spatial information that can be checked using the SAR image rather than being limited to point measurements only. Once the method was established

firmly for a drainage basin it would be tempting to go backwards and try to compute mean air temperature for the weather period just before image acquisition from the SAR data. Thereby within the field of climate monitoring ERS imagery could find an additional field of application.

7. ACKNOWLEDGEMENTS

This research was supported by the German Secretary of Science and Research (BMBF) within the programme 'Dynamic Processes in Antarctic Geosystems' (DYPAG) (Contract Number: 03PL016A), by the ESA pilot study 'Monitoring Of Dynamic Processes in Antarctic Geosystems' (MODPAG), (Contract Number: AO2.D149), and by the European Union 'Training and Mobility of Researchers' (TMR) programme 'Synergy of Remotely Sensed Data' (SYNERGY I) (Contract-Number: CHRX-CT93-0310). The authors would like to thank the Instituto Antarctico Argentino (IAA), the British Antarctic Survey (BAS) and the German Alfred-Wegener-Institut für Polar- und Meeresforschung (AWI) for their support in respect to logistics and field equipment. The authors are grateful for the invaluable assistance and discussions in the field by the Argentine and German collaborators.

8. REFERENCES

Braithwaite R J 1995, Aerodynamic stability and turbulent sensible-heat flux over a melting ice surface, the Greenland ice sheet, J. of Glac., Vol. 41, No. 139, pp 562 - 571.

Brutsaert W 1988, Evaporation in the Atmosphere, Dortrecht, London, 299 p.

Friedrich M 1996, Der Rückstreukoeffizient σ^0 für Schnee und Eis für aktive Fernerkundungssysteme im GHz-Bereich - Abhängigkeit und Berechnung, unpublished master thesis University of Freiburg, 70 p.

Parlow E 1996, Correction of terrain controlled illumination effects in satellite data, in: Parlow È (ed.), Progress in environmental remote sensing research and applications, Proc. of 15th EARSeL Symp., Basel 04 - 06 Sept. 1995, pp 139 - 145.

Reynolds J M 1981, The distribution of mean annual temperatures in the Antarctic Peninsula, British Antarctic Survey Bulletin, 54, pp. 123- 133.

Sanson J 1989, Antarctic surface temperature time series, J. of Climate, Vol. 2, pp. 1164 - 1172.

Schwerdtfeger W 1976, Changes of temperature field and ice conditions in the area of the Antarctic Peninsula, Monthly Weather Rev., Vol. 104, pp 1441 - 1443.

Vaughan D G & C S M Doake 1996, Recent atmospheric warming and retreat of ice shelves on the Antarctic Peninsula, Nature, Vol. 379, pp 328 - 330.

Wu X, K-H Thiel & S Wunderle 1996, The use of tandem data in the Antarctic area, ERS SAR Interferometry Workshop, University of Zurich, 30 Sept. - 23 Oct. 1996, 8 p.,
http://www.geo.unizh.ch/rsl/fringe96/papers/thiel-wu-1/

Wunderle S 1996, Die Schneedeckendynamik der Antarktischen Halbinsel und ihre Erfassung mit aktiven und passiven Fernerkundungsverfahren, Freiburger Geographische Hefte Nr. 48, University of Freiburg, 172 p.

Wunderle S & H Saurer 1995, Snow properties of the Antarctic Peninsula derived from ERS-1 SAR images, Proceedings of the 21st Annual Conference of the Remote Sensing Society 11th - 14th of September 1995, University of Southampton, pp 1231-1237.